Application of Homogenization Technique to Geometric Multigrid Method for Electromagnetic Finite Element Analysis

Tsubasa Kimura[1], Takeshi Mifune[2], and Tetsuji Matsuo[3], *Member, IEEE*

[1]Kyoto University, Kyoto, Japan, kimura@fem.kuee.kyoto-u.ac.jp
[2]Kyoto University, Kyoto, Japan, mifune@fem.kuee.kyoto-u.ac.jp
[3]Kyoto University, Kyoto, Japan, tmatsuo@kuee.kyoto-u.ac.jp

***Abstract*—The geometric multigrid method is an efficient solver for large sparse matrix equations arising in finite element analyses and is widely used to solve various electromagnetic problems. However, this method has difficulty in generating hierarchical computational grids for complicated geometries. Although using a structured mesh can mitigate this difficulty, it becomes an inconvenience for finite element analysis in practical cases. This paper proposes a homogenization technique for the geometric multigrid method, which resolves the difficulty in representing various geometries by simple grids. A sample analysis of the electrostatic field suggests the promising performance of the proposed method.**

***Index Terms*—Electromagnetic analysis, finite element methods, multigrid method.**

I. Introduction

Finite element (FE) analysis [1] is used widely to solve electromagnetic problems. Discretization of the electromagnetic equations by the FE method leads to a large sparse matrix equation. Because the cost of solving the matrix equation dominates the total computation cost of FE analysis, it is important to develop a fast and efficient matrix solver.

The geometric multigrid (GMG) method [2], [3] is known as an efficient solver for matrix equations arising in FE analysis. Although the GMG method is an $O(N)$ solver that uses hierarchical computational grids [2], implementing the GMG method involves the tedious tasks of generating and managing the hierarchical grids, which is particularly difficult in practical applications with complicated geometries. Although using structured grids [Fig. 1] reduces the difficulty significantly, this compromises the flexibility of the FE method to handle various geometries.

In this paper, we present a GMG solver combined with the interface homogenization (IH) technique [4]. The IH technique compensates for the lack of flexibility of the GMG method when using structured grids by allowing the grids to be unfitted to the material geometry or interface. When the GMG method is combined with the IH technique, the prolongation matrix [2] in the GMG algorithm should be determined by taking into account the refraction of the field at the unfitted interfaces, as described in Section III.

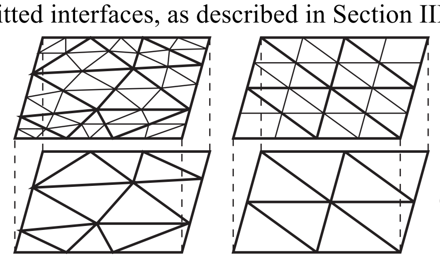

Fig. 1. Unstructured (left) and structured (right) hierarchical grids.

II. Basic Equations and Formulation

As a sample problem, consider the following 2D electrostatic problem:

$$-\nabla \cdot \epsilon \nabla V = \rho, \tag{1}$$

where ϵ, V, and ρ are the electric permittivity, the electric potential, and the electric charge density, respectively. Discretizing (1) by the FE method, we obtain the matrix equation

$$K\boldsymbol{a} = \boldsymbol{b}, \tag{2}$$

where K, $\boldsymbol{a}$, and $\boldsymbol{b}$ are the coefficient matrix, the unknown vector, and the right-hand side vector, respectively. The components of K are given by

$$[K]_{ij} = \int_\Omega \epsilon \nabla N_i \cdot \nabla N_j \, dS, \tag{3}$$

where N_i and N_j are first-order shape functions [1].

III. Multigrid Method with Homogenization

In this study, it is assumed that the analysis domain is discretized by the structured grids that are composed of isosceles right triangles [Figs. 1 and 3]. The capability of the present methodology, however, is not limited to cases using structured grids. The standard V-cycle [2] is adopted as the multigrid solver for (2).

When using structured grids, the geometries of the analyzed model or of the material interfaces are inevitably unfitted to the grids. The IH technique permits this situation without loss of accuracy [4]. The coefficient matrices in each level of the nested grids are given in the same way as (3).

Fig. 2 shows a triangular element of a coarse grid that is composed of four elements of a finer grid. In Fig. 2, the unfitted material interface, which is represented by a line within the element, is given by $l(x, y) = px + qy + r = 0$. The electric permittivity is given respectively by ϵ_+ and ϵ_- in the subregions $l > 0$ and $l < 0$. The coordinate values of each node of the coarser grid are denoted by (x_i, y_i), and we write $l_i = l(x_i, y_i)$. It is assumed without loss of generality that the placement of the nodes satisfies $l_1 \neq 0$, $l_1 l_2 \leq 0$, and

$l_1 l_3 \leq 0$.

In the conventional multigrid method, prolongation [2] onto the finer grid from the coarser one is done using the arithmetic mean of the values on the coarser grid, for example, $v_{12}^f = (v_1 + v_2)/2$. It is expected that this standard prolongation will not work for the unfitted elements. Hence, we propose a prolongation taking into account the refraction occurring at the interface of the different media.

The given values v_1, v_2, and v_3 can be regarded as the electric potential at each node of the coarser grid in Fig. 2. Assuming that the field that is uniform in each medium, the electric field can be written in the forms

$$\boldsymbol{E}_+ = c_n \boldsymbol{n} + c_t \boldsymbol{t} \text{ in } l(x,\ y) > 0, \tag{4}$$

$$\boldsymbol{E}_- = \frac{\epsilon_+}{\epsilon_-} c_n \boldsymbol{n} + c_t \boldsymbol{t} \text{ in } l(x,\ y) < 0, \tag{5}$$

where $\boldsymbol{n}$ and $\boldsymbol{t}$ denote $(p \quad q)^{\mathrm{T}}$ and $(-q \quad p)^{\mathrm{T}}$ respectively. The constants c_n and c_t are obtained below.

We have following simultaneous equations:

$$v_1 - v_2 = \frac{|l_1|}{|l_1|+|l_2|} \boldsymbol{E}_+ \cdot \boldsymbol{\Delta x_{12}} + \frac{|l_2|}{|l_1|+|l_2|} \boldsymbol{E}_- \cdot \boldsymbol{\Delta x_{12}}, \tag{6}$$

$$v_1 - v_3 = \frac{|l_1|}{|l_1|+|l_3|} \boldsymbol{E}_+ \cdot \boldsymbol{\Delta x_{13}} + \frac{|l_3|}{|l_1|+|l_3|} \boldsymbol{E}_- \cdot \boldsymbol{\Delta x_{13}}, \tag{7}$$

where $\boldsymbol{\Delta x_{12}} = (\Delta x_{12} \quad \Delta y_{12})^{\mathrm{T}} = (x_1 - x_2 \quad y_1 - y_2)^{\mathrm{T}}$ and $\boldsymbol{\Delta x_{13}} = (\Delta x_{13} \quad \Delta y_{13})^{\mathrm{T}} = (x_1 - x_3 \quad y_1 - y_3)^{\mathrm{T}}$. Solving the above equations, we obtain

$$c_n = A_{12}^n \Delta v_{21} + A_{13}^n \Delta v_{31}, \tag{8}$$

$$c_t = A_{12}^t \Delta v_{21} + A_{13}^t \Delta v_{31}, \tag{9}$$

where

$$\Delta v_{21} = v_2 - v_1, \Delta v_{31} = v_3 - v_1, \qquad (10), (11)$$

$$A_{12}^n = \frac{\beta_{13}(|l_1|+|l_2|)}{\alpha_{12}\,\beta_{13} - \alpha_{13}\beta_{12}}, A_{13}^n = -\frac{\beta_{12}(|l_1|+|l_3|)}{\alpha_{12}\,\beta_{13} - \alpha_{13}\beta_{12}}, \qquad (12), (13)$$

$$A_{12}^t = \frac{\alpha_{13}(|l_1|+|l_2|)}{\alpha_{13}\beta_{12} - \alpha_{12}\,\beta_{13}}, A_{13}^t = -\frac{\alpha_{12}(|l_1|+|l_3|)}{\alpha_{13}\beta_{12} - \alpha_{12}\,\beta_{13}}, \qquad (14), (15)$$

$$\alpha_{12} = \left(|l_1| + \frac{\epsilon_+}{\epsilon_-}|l_2|\right) \boldsymbol{n} \cdot \boldsymbol{\Delta x_{12}}, \tag{16}$$

$$\alpha_{13} = \left(|l_1| + \frac{\epsilon_+}{\epsilon_-}|l_3|\right) \boldsymbol{n} \cdot \boldsymbol{\Delta x_{13}}, \tag{17}$$

$$\beta_{12} = (|l_1| + |l_2|) \boldsymbol{t} \cdot \boldsymbol{\Delta x_{12}}, \tag{18}$$

$$\beta_{13} = (|l_1| + |l_3|) \boldsymbol{t} \cdot \boldsymbol{\Delta x_{13}}. \tag{19}$$

When $|l_1| \geq |l_2|$, the prolongation for v_{12}^f is obtained from

$$v_{12}^f - v_1 = \frac{1}{2} \boldsymbol{E}_+ \cdot \boldsymbol{\Delta x_{12}}, \tag{20}$$

or

$$v_{12}^f = \left(1 - \frac{1}{2}\left(\boldsymbol{n} \cdot \boldsymbol{\Delta x_{12}} (A_{12}^n + A_{13}^n) - \boldsymbol{t} \cdot \boldsymbol{\Delta x_{12}} (A_{12}^t + A_{13}^t)\right)\right) v_1 + \frac{1}{2}(\boldsymbol{n} \cdot \boldsymbol{\Delta x_{12}} A_{12}^n + \boldsymbol{t} \cdot \boldsymbol{\Delta x_{12}} A_{12}^t) v_2 + \frac{1}{2}(\boldsymbol{n} \cdot \boldsymbol{\Delta x_{12}} A_{13}^n + \boldsymbol{t} \cdot \boldsymbol{\Delta x_{12}} A_{13}^t) v_3. \tag{21}$$

When $|l_1| < |l_2|$, the prolongation is obtained from

$$v_2 - v_{12}^f = \frac{1}{2} \boldsymbol{E}_- \cdot \boldsymbol{\Delta x_{13}}. \tag{22}$$

We can obtain v_{13}^f in a similar way, and v_{23}^f is given by the arithmetic average of v_2 and v_3.

When triangular grids are used, each node to be interpolated belongs to two elements of the coarser grid. Because (21) (or (22)) with respect to these two elements may lead to different values, we adopt the arithmetic average of those values.

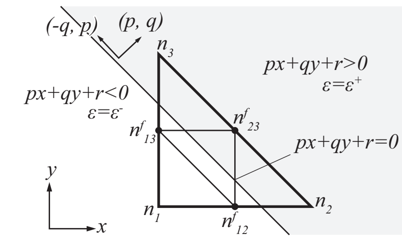

Fig. 2. Unfitted element of a coarse grid.

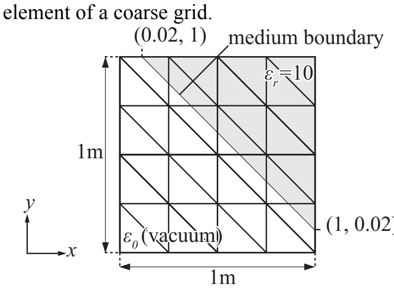

Fig. 3. Test model and an example of a structured mesh.

IV. Numerical Result

Fig. 3 shows the test problem, in which the analysis domain is discretized by 128 × 128 × 2 triangles. The Gauss–Seidel method is used as the smoother [2] and the LU decomposition is for the coarsest grid, which is the fifth coarse grid (that is, the total number of grids is six).

The Dirichlet conditions are imposed at the boundaries $y = 1.0$ m and $y = 0.0$ m (10 and 1 V, respectively). The GMG iteration is terminated when the relative residual norm becomes less than 10^{-8}. In model 1, the entire analysis field is a vacuum. In model 2, the relative permittivity is set to 10 for $l > 0$ and to 1 for $l \leq 0$. Note that unfitted elements arise in model 2.

Table 1 shows the number of iterations required for convergence of the GMG method. Convergence of the GMG method with the conventional prolongation becomes slow when unfitted elements arise. In contrast, using the proposed prolongation maintains the rapid convergence of the GMG method, even with unfitted elements.

The GMG method presented in this study is both flexible at handling various geometries and converges rapidly. More practical applications will be reported in the full paper.

TABLE I

Numerical Result: Number of Iterations.

ε_r	Conventional method	Proposed method
1	10	11
10	28	11

V. References

[1] J. Jin, *The Finite Element Method in Electromagnetics*, 2nd. Ed., John Wiley & Sons, Inc., 2002.

[2] Y. Zhu and A.C. Cangellaris, *Multigrid Finite Element Methods for Electromagnetic Field Modeling*, IEEE Press, Piscataway, 2006.

[3] S. Odawara, Y. Gao, and K. Muramatsu, "Magnetic Field Analysis With Nonconforming Voxel Modeling Using the Nested Geometric Multigrid Method," *IEEE Trans. Magn.*, vol. 48, no. 2, pp. 595-598, Feb. 2012.

[4] T. Mifune, "Interface Homogenization Technique for Unfitted Finite Element Electromagnetic Analysis," *IEEE Trans. Magn.,* to be published.